

Susceptibility of a Simple Transmission Line Inside an Enclosure Against Normal Incident Plane Wave

S. Abadpour¹, P. Dehkhoda², R. Moini¹, S. H. H. Sadeghi¹ and H. R. Karami³

¹ Department of Electrical Engineering
AmirKabir University of Technology, Tehran 15875-4413, Iran
sevda.abadpour@aut.ac.ir, moini@aut.ac.ir, sadeghi@aut.ac.ir

² Institute of Communications Technology and Applied Electromagnetics
AmirKabir University of Technology, Tehran 15875-4413, Iran
pdehkhoda@aut.ac.ir

³ Department of Electrical Engineering
Bu-Ali Sina University, Hamadan 65178, Iran
hamidr.karami@basu.ac.ir

Abstract — In this paper, susceptibility of a Microstrip Transmission Line (MTL) as a simple Printed Circuit Board (PCB) against a normal incident plane wave is studied. Here, the induced voltage on the open port of the MTL is considered as the susceptibility criterion for the MTL. Two different approaches are applied: the Method of Moments (MoM) and the Finite Integration Technique (FIT). In addition to simulations, we performed measurements inside a semi-anechoic chamber. Both simulations show very good agreement with the measurements. In addition to frequency domain results, time domain induced open circuit voltage is calculated. The effect of different aperture sizes on the susceptibility of a shielded MTL is examined. It is shown that large apertures can multiply the disagreeable effect of the interfering wave on the MTL, compared to the case where no shield is utilized.

Index Terms - Finite Integral Technique (FIT), Method of Moments (MoM), microstrip transmission line susceptibility, shielding enclosure and susceptibility measurements.

I. INTRODUCTION

Failure and malfunction of electronic systems that are sensitive to electromagnetic disturbances is becoming a serious problem [1]. The

malfunctioning of an electronic system can be related to its susceptibility to an external electromagnetic field. As defined in [2], susceptibility is a relative measure of a device or a system's propensity to be disrupted or damaged by Electromagnetic Interference (EMI) exposure to an incident field.

The radiated susceptibility of a Printed Circuit Board (PCB) influenced by an external electromagnetic field can be a criterion to determine the susceptibility of a whole electronic device. The induced interference signal on the traces of a PCB causes partial functional failures or even irreversible damages; depending on the shape and amplitude of the interference signal as well as the trace properties. Different numerical methods such as Method of Moments (MoM) and Finite Element Method (FEM) have been utilized to evaluate the susceptibility of a bare PCB [3-6]. On the other hand, in order to measure susceptibility of a PCB, different test cells are used, such as a transverse Electromagnetic Transmission Cell (TEM cell) [7], an Asymmetric Transverse Electromagnetic Transmission cell (ATEM cell) [8], Gigahertz Transverse Electromagnetic Transmission cell (GTEM cell) [6,9] and reverberating chamber [10]. In those measurements, an unshielded PCB is examined and the induced voltage on different parts of the

PCB is defined as the susceptibility of the circuit. Generally speaking, metallic enclosures are widely used to hinder electromagnetic leakage from electronic equipment and also to reduce the susceptibility of the sensitive devices against external interference. Numerous techniques have been utilized to evaluate the SE of perforated empty [11-14] and also loaded enclosures [15-19]. In most practical applications, Shielding Effectiveness (SE) and consequently the susceptibility of a PCB inside the enclosure are primarily affected by the apertures perforated to accommodate visibility, ventilation or access to interior components [20].

In this paper, susceptibility of a typical Microstrip Transmission Line (MTL) as a simple PCB enclosed within a perforated cavity is studied. To this end, two different numerical methods are utilized. For a MTL with air cushion, an efficient MoM code is developed to solve the governing Electric Field Integral Equation (EFIE), with the well-known Rao–Wilton–Glisson (RWG) basis functions [10] for the unknown electric currents on the surface of the enclosure. The second approach is the Finite Integration Technique (FIT) by CST, the well-known commercial software that solves the problem of MTL with dielectric substrate. By evaluating the electric field at the open port of the MTL, the induced open circuit voltage (V_{oc}) as the determinant parameter for MTL susceptibility is calculated.

In addition to simulations, Electromagnetic Susceptibility (EMS) measurements have been performed for different shielded and unshielded MTLs inside a semi-anechoic chamber. To the knowledge of the authors, it is for the first time that EMS test of a PCB inside a semi-anechoic chamber with an interference producing antenna is reported. This setup has been used frequently for SE measurements of empty enclosure [13,18]. It will be shown that measurements are in very good agreement with the simulation results. In this paper, the main goal is to study the susceptibility of a shielded MTL at resonant frequencies of the enclosing perforated enclosure; thus, for the considered enclosure, measurements are performed at 500-1000MHz.

In addition to frequency domain results, time domain induced voltage on the open port of the MTL caused by a Gaussian plane wave is

calculated. It will be shown that using the enclosure with a large aperture not only does not protect the MTL against the interfering wave, but also decrease the immunity of the MTL.

This paper is organized as follows: section II reviews the employed numerical solution methods. Then the measurement setup is described. Section III studies the effect of different aperture sizes on the immunity of a shielded MTL. Also, time domain results are discussed. A brief conclusion is presented in section IV.

II. THEORY

Here, the RWG-MoM technique is chosen to solve the governing EFIE in the problem of a shielded MTL with air cushion. A MATLAB code is developed on a Core™ i7-2600 CPU @ 3.4 GHz, with 8 GB of RAM. For the MTL with dielectric substrate, CST software is utilized. Both simulations are compared with the measurements. A brief formulation for RWG-MoM and FIT are found in sub-section A and B, respectively. In subsection C, experimental setup is introduced and the open voltage calculation from the measured data is presented.

A. MoM approach

A rectangular metallic cube with interior dimensions of $a \times b \times c$ and wall thickness of d is illustrated in Fig. 1. A rectangular aperture with length L and width W is located at the center of the cavity's illuminated surface.

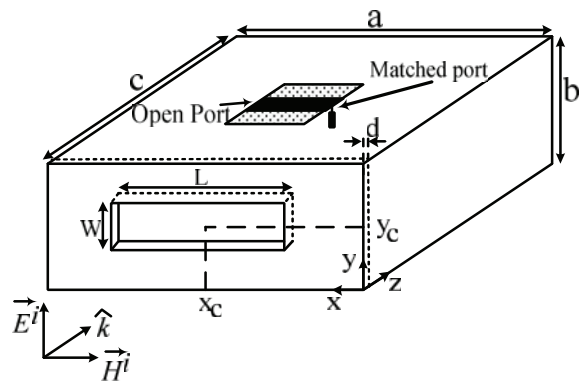


Fig. 1. Geometry of problem.

The incident plane wave is \vec{E}^i and the MTL is placed inside the enclosure. The MTL is matched at one port and is open at the other port.

According to physical equivalence theorem [21], incident wave induces an electric current \vec{J} on the metallic parts of the structure. The scattered fields (\vec{E}^s, \vec{H}^s) by \vec{J} are calculated at any point inside or outside the enclosure by [21]:

$$\vec{E}^s = -j\omega\mu \oint\!\!\!\oint \vec{J} G(r, r') ds' - \frac{j}{\omega\epsilon} \oint\!\!\!\oint (\vec{\nabla} \cdot \vec{J}) \vec{\nabla}_r G(r, r') ds', \quad (1)$$

$$\vec{H}^s = \frac{1}{\mu} \nabla \times \vec{A} = \frac{-1}{4\pi} \oint\!\!\!\oint \vec{J} \times G(r, r'), \quad (2)$$

where $G(r, r')$ is the free space of Green's function, and

$$\vec{\nabla}_r G(r, r') = \frac{\partial}{\partial r} (G(r, r')) = \frac{\partial}{\partial R} (G(r, r')) \times \frac{\partial R}{\partial r} = \frac{-e^{-jkR}}{4\pi R} \left(jk + \frac{1}{R} \right) \hat{R}. \quad (3)$$

Applying the boundary condition on the perfect metallic parts of the structure, an EFIE is obtained. Afterward, \vec{J} is expanded by RWG basis functions on the triangular shaped discretization [22]. The resultant integral equation is then solved by MoM. Detailed study on RWG-MoM solution is presented in [22]. Having the coefficients of \vec{J} on the meshes and re-using (1)-(3), the scattered electromagnetic field at any point is achieved. By integrating the obtained total electric field along the length of the MTL open port, V_{oc} is calculated. Please note that if no dielectric with permittivity constant larger than 1 is used in the problem, there is no limitation on the shape of the enclosure, the aperture or the MTL in the applied method. To this end, air substrate is used for the MTL. In order to consider the wall thickness, the aperture surrounding walls and the enclosure, internal and external walls should be discretized.

B. FIT method

Maxwell's equations can be applied in their integral form to the cells of a discretized problem [23,24]. This approach is the basis of the Finite Integration Technique (FIT) that is found to be a suitable numerical method for analyzing electromagnetic problems, due to its high flexibility as well as its ability to deal with arbitrary material distributions, geometrical modeling, curved boundaries and complex shapes. In homogeneous media, the discretization method of FIT is similar to the FDTD method. However, the FIT transforms Maxwell's equations in their integral form to a linear system of equations. This

technique treats interfaces between different media in a more accurate manner [24].

Various approaches based on an adaptive mesh, the sub-gridding, the Conformal FIT (CFIT) and Non-Orthogonal Grids (NFIT) have been introduced to overcome staircase approximation. A finer mesh can be used only in sections where higher accuracy is required by employing adaptive mesh approaches; therefore, this reduces the number of grid points in the whole simulation area [23,24]. The powerful Computer Simulation Technology (CST) commercial software is a developed code based on FIT method.

In this paper, CST is used to analyze the susceptibility of shielded and unshielded MTLs with air and dielectric substrates. Respectively, 172, 260 and 1,163,264 mesh cells are required to obtain convergent results for the unshielded and shielded MTL with dielectric substrate. For the MTL with air cushion, necessary mesh cells are 284,026 and 1,608,576 for the unshielded and shielded, respectively. The high number of meshes in the shielded case is due to the relatively small size of MTL when compared to the large size of the enclosure.

C. Experimental setup

Measurements are performed inside a semi-anechoic chamber using a horn antenna as the source of interference. The antenna is placed 2 m away from the MTL (shielded or unshielded) in its line of sight, as shown in Fig. 2, to satisfy the far field region requirement. The absorbers are put between the antenna and the MTL to remove the reflection from the floor.

Figure 3 shows a schematic of the measurement setup. A Vector Network Analyzer (VNA) is used to measure the scattering parameters. The VNA is placed outside of the anechoic chamber and its port 1 is connected to the antenna. MTL is connected to VNA port 2 at one side and at the other side it is matched.

In order to calculate the induced V_{oc} on the MTL from the measurement results, the measured scattering parameters are related to the open circuit voltage by [25]:

$$V_{oc} = \frac{2S_{21}}{(1-S_{11})(1-S_{22})-S_{12}S_{21}} I_1, \quad (4)$$

where I_1 is calculated from the known injected power by the VNA into its port 1 and its 50 Ω

characteristic impedance, neglecting the reflection from the antenna. We set the power of the VNA at its port 1 in a way that the incident field amplitude at the enclosure exposed wall to be 1 V/m. For calculating the necessary power, loss of cables, gain of the antenna and the distance between antenna and the enclosure's perforated wall is considered.



Fig. 2. Experimental setup of test.

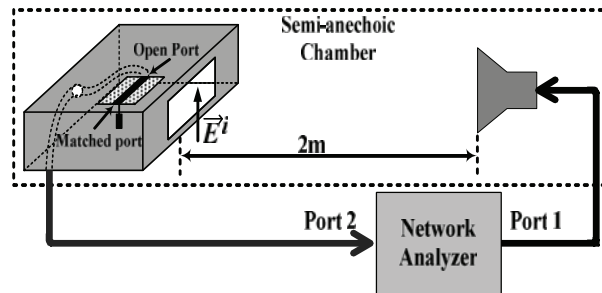


Fig. 3. Schematic of setup test.

III. RESULTS

A. Frequency domain analysis

Utilized shielding enclosure is a $30 \times 12 \times 30$ cm³ box with one 18×5 cm² aperture in the illuminated wall. Two different MTLs are examined. The first one has 3.18 mm air substrate with trace width and length of 15.6 mm and 74.9 mm, respectively (Fig. 4 (a)). Since there is no dielectric in this MTL, it is suitable to be analyzed by the developed RWG-MoM code. The second one is a more practical MTL with RO4003 substrate with trace length and width of 45 mm and 1.12 mm, respectively (Fig. 4 (b)). Both are designed to have the characteristic impedance of

50 Ohm at 1 GHz. They are matched at one port and open at the other port.

The MTL is placed inside the enclosure 15 cm away from the front panel, horizontally in a way that the transmission line is perpendicular to the front wall. In the case where the shield is not used, the MTL is placed at the same location as the shielded case.

The effect of an incident plane wave on the MTL of Fig. 4 (a) is studied for two cases; shielded and unshielded. The incident electric field is polarized along y-direction and its amplitude is 1 V/m. V_{oc} is calculated by developed RWG-MoM code and is compared with CST results and measurements in Fig. 5 for unprotected and protected cases. It is clear that a very good agreement exists between the results. As observed, using the mentioned enclosure with 18×5 cm² aperture not only does not decrease the effect of impinging wave, but also raise the V_{oc} up to 3 times more at some frequencies.

To investigate this undesirable effect more, SE of the considered empty enclosure at its center point is calculated by CST and depicted in Fig. 6 for different aperture sizes. Please note that SE is the ratio of the field strength in the presence and absence of the enclosure at one point inside the enclosure and is defined for a shielding enclosure to show its ability to hinder the electromagnetic fields. As observed, as the aperture size increases, the bandwidth at which SE is less than zero becomes larger. Negative SE (dB) means that the level of electromagnetic field is intensified at the considered point. This happens at resonant frequencies of the enclosure with the aperture. Clearly, increasing the aperture size would decrease the Q factor of the structure and therefore the bandwidth at which SE (dB) is negative, increases. In this case, shield acts conversely and amplifies the effect of interfering wave on the MTL. Please note that for small apertures, such as 5×0.5 cm² in Fig. 6, shield behavior is improved significantly and SE does not have negative values.

To further study the effect of aperture size on the susceptibility of the shielded MTL, the induced voltage on the open port of the MTL with air cushion inside the enclosure is depicted in Fig. 7. The disagreeable effect of large aperture size is clarified in this figure.

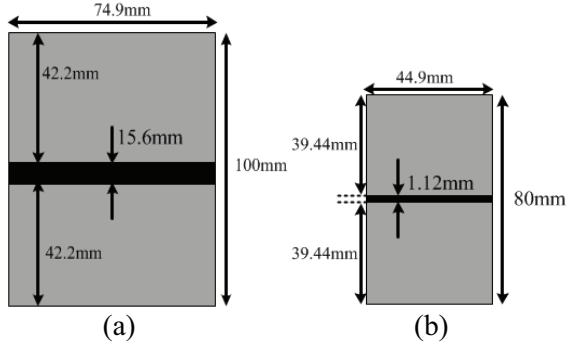


Fig. 4. Top view of MTL with: (a) air substrate and (b) with dielectric substrate.

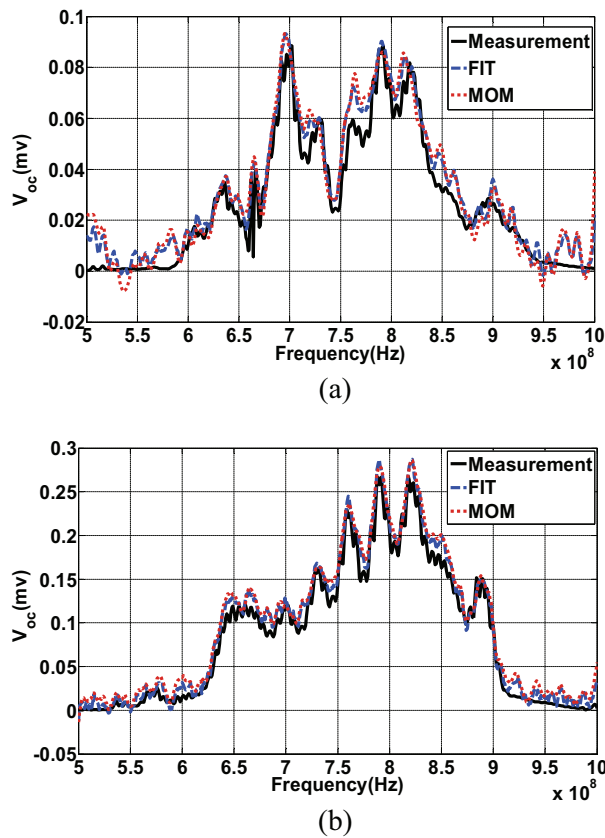


Fig. 5. Induced voltage on the open port of the MTL with air cushion of Fig. 4 (a); measurements, CST and our developed MoM for: (a) unshielded and (b) shielded cases.

As observed, aperture size of $18 \times 5 \text{ cm}^2$ allows large MTL open port voltage at a wide frequency range (250 MHz), while the effect of $10 \times 5 \text{ cm}^2$ aperture is limited to a small frequency band (45 MHz). Please note that for the case of very small aperture ($5 \times 0.5 \text{ cm}^2$) the induced open port voltage

is negligible. This behavior has already been predictable by considering the SE in Fig. 6.

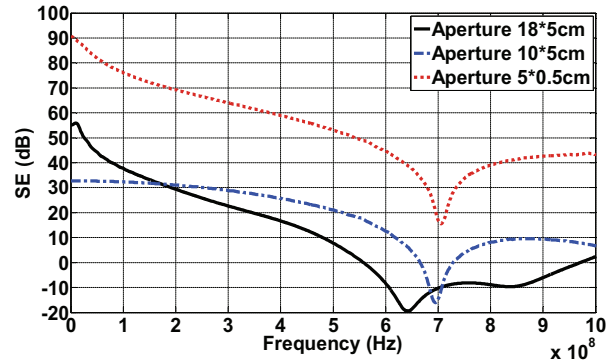


Fig. 6. SE comparison for the $30 \times 12 \times 30 \text{ cm}^3$ empty enclosure with different apertures; CST simulations.

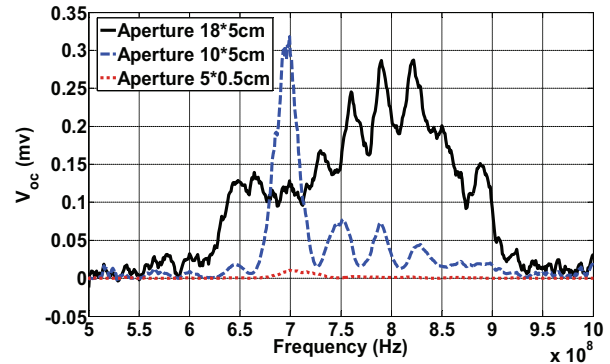


Fig. 7. V_{oc} at the open port of the MTL of Fig. 4 (a), inside the $30 \times 12 \times 30 \text{ cm}^3$ enclosure with different apertures; CST simulations.

In addition to MTL with air cushion, an MTL with RO4003 substrate (Fig. 4 (b)) is studied using CST as the simulation tool. Figure 8 compares the calculated V_{oc} and the measurements. A very good agreement between the results is clear in the figure. As observed, using the shield does not have a significant effect on reducing the induced V_{oc} on the MTL and the maximum value of V_{oc} for shielded and unshielded cases remains the same, occurring at different frequencies. Please be reminded that for the MTL with air cushion, the induced V_{oc} was multiplied when the shield was used. It means dielectric substrate with permittivity more than 1 can maintain the immunity of the MTL in an enclosure with large aperture, in the order of the unshielded case. As an

ending conclusion, using an enclosure with large apertures to protect systems against electromagnetic interference degrades the immunity of the system and should not be used definitely.

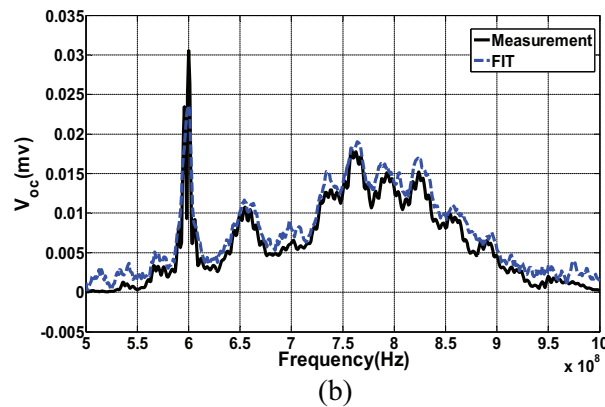
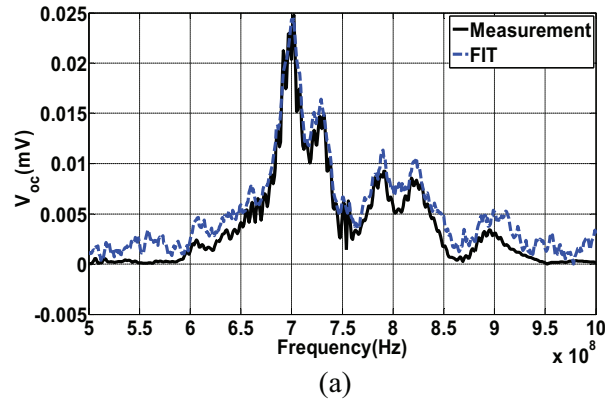


Fig. 8. Induced voltage on the open port of MTL with RO4003 substrate of Fig. 4 (b) by measurements and CST: (a) unshielded MTL and (b) shielded MTL.

B. Time domain analysis

Time domain results can be calculated by applying an Inverse Fourier Transform (IFFT) on the frequency domain data [26]. To this end, first, the interfering time domain signal should be transformed to frequency domain. Figure 9 illustrates a frequency domain, Gaussian plane wave with the center frequency of 750 MHz. The considered enclosure, MTLs and their location are the same as described in the previous sub-section. For the aperture size of 18×5 cm², time-domain V_{oc} for both MTLs of Figs. 4 (a) and (b) is depicted in Figs. 10 and 11, respectively. Please note that IFFT is implemented with 512 points.

As observed in Figs. 10 and 11, the level of the induced voltage on the shielded MTL is larger than the case where no shield is used.

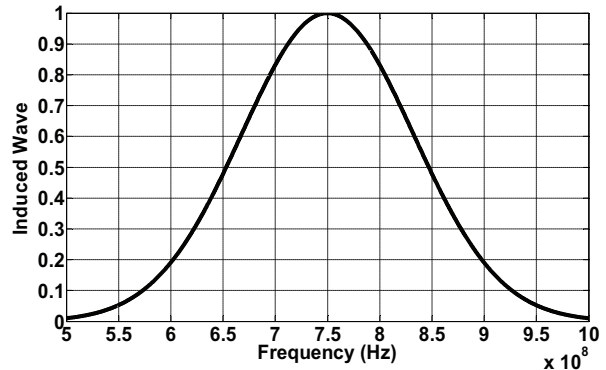


Fig. 9. Gaussian incident plane wave.

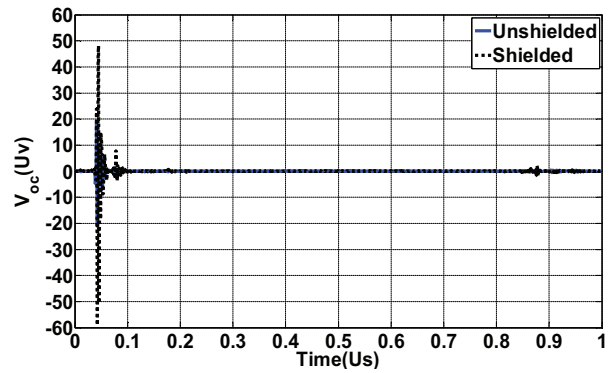


Fig. 10. Time domain V_{oc} comparison for shielded and unshielded MTL with air cushion of Fig. 4 (a).

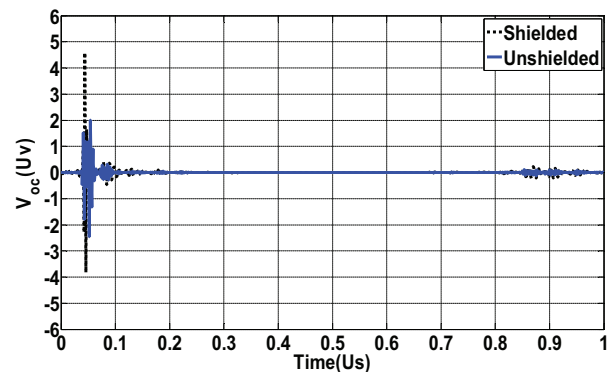


Fig. 11. Time domain V_{oc} comparison for shielded and unshielded MTL with RO4003 substrate of Fig. 4 (b).

In order to be able to compare the time domain results, Root Mean Square (RMS) value of the

induced V_{oc} is considered. RMS voltage is obtained according to [27] by:

$$V_{oc}^{rms} = \sqrt{\frac{\sum_{i=0}^n (V(t_i))^2}{n}}, \quad (5)$$

where $V(t_1)$, $V(t_2)$, ..., and $V(t_n)$ are the induced voltages at n time instances of t_1 , t_2 , ..., t_n . Table 1 compares the RMS V_{oc} values for the shielded and unshielded MTLs of Fig. 4.

Table 1: RMS value of induced time domain V_{oc} for the shielded and unshielded MTLs

| | V_{oc}^{rms} (μ v) Shielded case | V_{oc}^{rms} (μ v) Unshielded case | $\frac{V_{oc}^{rms}(shielded)}{V_{oc}^{rms}(unshielded)}$ |
|------------------------------------|--|--|---|
| MTL with air caution | 3.4397 | 1.0724 | 3.21 |
| MTL with RO4003 substrate | 0.2337 | 0.1583 | 1.48 |

As compared in the table, V_{oc}^{rms} of the shielded MTLs is higher than the case where no shield is used. In addition, the ratio of V_{oc}^{rms} for the MTL with air cushion (3.21) is about 2 times larger than that of the MTL with RO4003 substrate (1.48). It is also worth noting that for any case (shielded or unshielded) the induced V_{oc}^{rms} on the MTL with air cushion is larger than that on the MTL with dielectric substrate; i.e., the MTL with air cushion is more susceptible to the external field.

IV. CONCLUSION

In this paper, susceptibility of a matched MTL against an interfering plane wave is studied. The induced voltage on the open port of the MTL is considered as a measure for the MTL susceptibility. Two different cases are considered; once the bare MTL is illuminated by the interfering field and then in order to hinder electromagnetic wave, the MTL is placed inside a shielding enclosure. Two MTLs with air cushion and RO4003 substrate were studied. For the MTL with air substrate, a RWG-MoM solution code was developed, while for the MTL with dielectric substrate, CST simulation was applied.

Both simulations were validated by the measurements performed in an anechoic chamber.

It was shown that a large size aperture degrades susceptibility of the MTL at a large bandwidth compared to the case where no shield is used. As the aperture size is reduced, SE improves and this disagreeable effect decreases. However, at the enclosure resonance bandwidth, care should be taken of the immunity of the MTL, especially when the aperture size is large.

In addition, it was observed that for the MTL with dielectric substrate, maximum induced voltage remained the same as the case where no shield was used; however, a shift occurred in the frequency of the maximum voltage. For the MTL with air cushion, the induced voltage was very larger than that induced to the bare MTL.

In addition, the time domain effect was studied for an incident Gaussian wave on the shielded and unshielded MTLs.

REFERENCES

- [1] R. P. Clayton, "Introduction to electromagnetic compatibility," *John Wiley & Sons Inc.*, 2006.
- [2] I. M. Mark and M. N. Edward, "Testing for EMC compliance, approaches and techniques," *John Wiley & Sons Inc.*, 2004.
- [3] Y. Rousset, V. Arnautovski-Toseva, C. Pasquier, K. E. K. Drissi, and L. Grcev, "Using feko software for analysis of radiated electric field by power converters," *22nd Annual Rev. of Prog. In Applied Computational Electromagnetics (ACES Conf.)*, Miami, USA, pp. 881-888, March 2006.
- [4] F. Grassi, G. Spadacini, F. Narliani, and A. S. Pignari, "The use of feko for the modeling of test set-up for radiated susceptibility," *23rd Annual Rev. of Prog. In Applied Computational Electromagnetics (ACES Conf.)*, Verona, Italy, pp. 279-284, March 2007.
- [5] A. Nejadpak and O. A. Mohammed, "Finite element physics based modeling of cross-talk effect on PCB traces," *28th Annual Rev. of Prog. In Applied Computational Electromagnetics (ACES Conf.)*, Columbus, Ohio, pp. 768-773, April 2012.
- [6] M. Leone, "Radiated susceptibility on the printed-circuit-board level: simulation and measurement," *IEEE Trans. On EMC*, vol. 47, no. 3, pp. 471-478, 2005.
- [7] S. Atrous, D. Baudry, E. Gaboriaud, A. Louis, B. Mazari, and D. Blavette, "Near-field investigation of the radiated susceptibility of printed circuit boards," *Proc. IEEE Int. Symp. on Electromagnetic Compatibility-EMC Europe*, Detroit, USA, pp. 1-6, September 2008.
- [8] D. Jing and H. Guo, "Study on coupling characteristics for EM pulse into slotted shell of

- loaded PCB,” *Proc. IEEE Int. Conf. on Computer, Mechatronics, Control and Electronic Engineering (CMCE)*, HongGuo, China, pp. 398-401, August 2010.
- [9] L. Tian-Hong and M. J. Alexander, “A method to minimize emission measurement uncertainty of electrically large EUTs in GTEM cells and FARs above 1 GHz,” *IEEE Trans. On EMC*, vol. 48, no. 4, pp. 634-640, 2006.
- [10] H. Tarhini, M. E. Haffar, C. Guiffaut, G. Andrieu, A. Reineix, B. Pecqueux, and J. C. Joly, “Susceptibility of printed circuit boards in complex electromagnetic environment,” *Proc. IEEE Int. Symp. on Electromagnetic Compatibility-EMC Europe*, Detroit, USA, pp. 1-4, September 2008.
- [11] T. Namiki and K. Ito, “Numerical simulation using ADI-FDTD method to estimate shielding effectiveness of thin conductive enclosures,” *IEEE Trans. on Microwave Theory and Techniques*, vol. 49, no. 6, pp. 1060-1066, 2001.
- [12] J. Chen and J. Wang, “A three-dimensional semi-implicit FDTD scheme for calculation of shielding effectiveness of enclosure with thin slots,” *IEEE Trans. On EMC*, vol. 49, no. 2, pp. 354-360, 2007.
- [13] P. Dehkhoda, A. Tavakoli, and R. Moini, “Shielding effectiveness of a rectangular enclosure with finite wall thickness and rectangular apertures by the generalized modal method of moment,” *IET Science, Measurement and Technology*, vol. 3, no. 2, pp. 123-136, 2009.
- [14] M. Khorami, P. Dehkhoda, R. Moini, and H. H. S. Sadeghi, “Fast shielding effectiveness calculation of metallic enclosures with apertures using a multi-resolution method of moments technique,” *IEEE Trans. On EMC*, vol. 52, no. 1, pp. 230-235, 2010.
- [15] S. Yenikaya and A. Akman, “Hybrid MOM/FEM modeling of loaded enclosure with aperture in EMC problems,” *International Journal of RF and Microwave Computer-Aided Engineering*, vol. 19, no. 2, pp. 204-210, 2009.
- [16] B. Audone and M. Balma, “Shielding effectiveness of slots in rectangular cavities,” *IEEE Trans. On EMC*, vol. 31, no. 1, pp. 102-106, 1989.
- [17] D. W. P. Thomas, A. C. Denton, T. Konefal, T. Benson, C. Christopoulos, J. F. Dawson, A. Marvin, S. J. Porter, and P. Sewell, “Model of the electromagnetic field inside a cuboidal enclosure populated with conducting planes or printed circuit boards,” *IEEE Trans. On EMC*, vol. 43, no. 2, pp. 161-169, 2001.
- [18] K. Murano, T. Sanpei, F. Xiao, C. Wang, Y. Kami, and J. L. Drewniak, “Susceptibility characterization of a cavity with an aperture by using slowly rotating EM fields: FDTD analysis and measurements,” *IEEE Trans. On EMC*, vol. 46, no. 2, pp. 169-177, 2004.
- [19] C. Feng and Z. Shen, “A hybrid FD–MoM technique for predicting shielding effectiveness of metallic enclosures with apertures,” *IEEE Trans. On EMC*, vol. 47, no. 3, pp. 456-462, 2005.
- [20] S. Abadpour, P. Dehkhoda, H. R. Karami and R. Moini, “Aperture size effect on the susceptibility of a PCB inside an enclosure,” *IEEE Int. Conf. on Electromagnetics in Advanced Applications*, Torin, Italy, pp. 741-744, September 2011.
- [21] R. F. Harrington, “Time harmonic electromagnetic fields,” *McGraw-Hill*, New York, 1961.
- [22] S. M. Rao, D. R. Wilton, and A. W. Glisson, “Electromagnetic scattering by surfaces of arbitrary shape,” *IEEE Trans. On Antennas and Propagation*, vol. 30, pp. 409-418, 1982.
- [23] T. Weiland, “A discretization method for the solution of Maxwell's equations for six-component fields,” *Electronics and Communication (AEÜ)*, vol. 31, pp. 116, 1977.
- [24] Z. Rahimi, “The finite integration technique (FIT) and the application in lithography simulation,” *Technical Department, University of Erlangen-Nuremberg*, Ph.D., 2011.
- [25] D. M. Pozar, “Microwave engineering,” *Wiley*, 2005.
- [26] J. G. Proakis and D. K. Manolakis, “Digital signal processing, principles, algorithms and applications,” *Prentice Hall*, 2006.
- [27] A. V. Oppenheim, R. W. Schaffer, and J. R. Buck, “Discrete-time signal processing,” *Prentice-Hall*, 1999.